A Pulse-Front-Tilt–Compensated Streaked Optical Spectrometer with High Throughput and Picosecond Time Resolution

Introduction

Time-resolved spectroscopy, using an optical spectrometer coupled to a streak-camera recording system, is a common diagnostic technique in the field of short-pulse laser physics research. Streaked spectrometers analyze a point-source input by aligning the dispersed output of the spectrometer to the input slit of a streak camera. These instruments are particularly effective for single-shot experiments requiring detailed measurements of optical spectra with temporal resolutions of the order of picoseconds to nanoseconds. The overall temporal resolution of such instruments depends on the streak camera's performance and the configuration of the spectrometer used. For many demanding applications, a streaked-spectrometer instrument must have high spectral and temporal resolution while maintaining large optical throughput. These three parameters are intrinsically linked and the ability to simultaneously optimize them is limited. This article presents a novel technique that decouples throughput considerations from the spectral- and temporal-resolution optimization process.

Background of Pulse-Front Tilt

Pulse-front tilt (PFT) is a time-shearing effect inherent to angular dispersion in which the arrival time of light varies linearly with position across the beam in the plane of dispersion.[1,2] PFT can be explained geometrically by examining the path-length difference introduced across the beam at a dispersive interface (Fig. 147.35). In the case where a diffraction grating is used to generate angular dispersion, the total PFT after dispersion is given by

$$\Delta t = Nm\lambda / c, \tag{1}$$

where N is the total number of illuminated grating groves, m is the grating order used, λ is the wavelength of light, and c is the speed of light. An important quantity in spectrometer design is the angular dispersion that relates the change in angle of diffraction β to the change in wavelength and is given by

$$d\beta / d\lambda = mG / \cos(\beta). \tag{2}$$

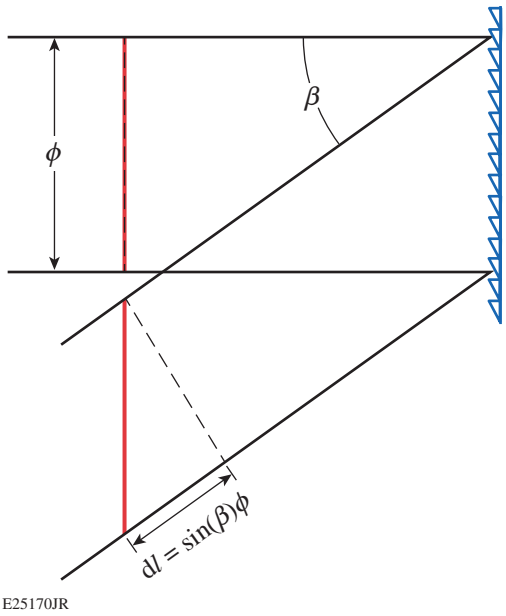

Figure 147.35
Pulse-front tilt (PFT) is introduced by the path-length asymmetries of a beam exiting an angularly dispersive medium. The total PFT increases with beam diameter and angular dispersion.

Combining Eqs. (1) and (2), and relating N to the beam diameter ϕ and groove density G, produces an expression that illustrates the difficulty of designing a spectrometer with high spectral resolution, good temporal resolution, and large throughput:

$$\Delta t = \frac{\phi\lambda\cos(\beta)}{c}\frac{d\beta}{d\lambda}. \tag{3}$$

For a given angular dispersion, attempts to improve throughput by increasing the size of the collection optic will result in a loss of temporal resolution.

Spectral- and Temporal-Resolution Limitations

The size of an individual spectral-resolution element can be defined as the product of the instrument's spatial impulse response multiplied by the linear dispersion ($\delta\lambda = \Delta x\, d\lambda/dx$). The linear dispersion ($d\lambda/dx$) is the product of the angular

dispersion and the output image's focal length. The imaging performance of the spectrometer, the point-spread function (PSF_{SC}) of the streak camera, and the size of the input object's image (wM) all contribute to the spatial impulse response. Adding these terms in quadrate gives

$$\Delta x^2 = (wM)^2 + PSF_{geo}^2 + PSF_{dif}^2 + PSF_{SC}^2, \qquad (4)$$

where w is the size of the input object, M is the magnification of the spectrometer along the axis of dispersion, and PSF_{geo} and PSF_{dif} are the geometric and diffractive limitations, respectively, of the spectrometer imaging optics. It is worth noting that, for a fixed collection aperture, attempts to improve spectral resolution by using a longer output focal length will increase M if asymmetric conjugates are used or will increase PFT if symmetric conjugates are used.

Three main mechanisms generally limit the temporal resolution of a streak camera: (1) the line-spread transit (LST) time, (2) electron transit time spread (TTS), and (3) space-charge broadening. LST is defined as the time it takes the sweep to traverse the width of a static cathode image and can be reduced by using a fast sweep rate and a narrowly focused cathode image. TTS arises because electrons generated at the photocathode have a distribution of initial velocity vectors and do not take the same amount of time to reach the phosphor output screen. TTS can be decreased by reducing the overall transit time or narrowing the excess electron energy distribution through judicious choice of photocathode material and/or signal wavelengths. Space-charge broadening is caused by the repulsive force felt from neighboring photoelectrons as they travel down the tube. Space-charge broadening spoils the image of the cathode and effectively increases the achieved LST. This effect can be managed by keeping the total electron-current density below an experimentally determined threshold level.

Segmented Spectrometer Design

Using a rectangular mask to limit the beam size and, therefore, the total number of grooves illumined at the grating surface is a viable technique to decrease total PFT.[3] While simple and effective, this method reduces system throughput and is not suitable for low-signal applications. Additionally, decreasing the beam size increases the imaging f number. When taken to the extreme, the masked aperture generates a large diffraction-limited spot size that spoils the instrument's spectral resolution. This result is consistent with the concept that spectral resolving power is directly proportional to the number of illuminated grating grooves.

A new type of spectrometer layout is proposed that uses the concept of a masked grating aperture to improve temporal resolution but maintains the throughput of an unmasked system. This is accomplished by breaking the full-aperture beam into a series of discrete rectangular segments. Each segment is prescribed an appropriate amount of delay, such that after the beam exits the dispersive medium, the individual segments are temporally aligned. Figure 147.36 shows how a transmission echelon optic is used to generate the required delay profile to compensate the overall PFT. The residual PFT is only what is accumulated across a single segment. The temporal delay between each segment is determined by the step height of the echelon optic and is set to be equal to the total PFT of a single segment. The practical limitations to the minimum echelon step width are the same as for a masked spectrometer. The echelon step width is minimized until the diffraction-limited spot size is comparable to the other contributing terms in the spectrometer's PSF.

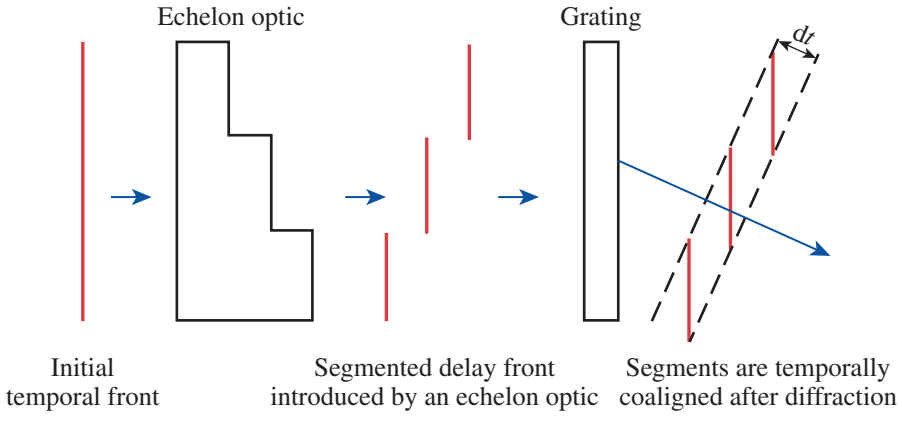

Figure 147.36
PFT can be reduced with no loss to throughput by segmenting the incoming beam into multiple sub-elements that are individually delayed to compensate for the path-length difference introduced by the diffraction grating. The residual PFT is limited to the accumulation across a single segment and the overall temporal resolution is improved by a factor equal to the number of sub-elements used.

Spectrometer Design

A prototype segmented spectrometer (Fig. 147.37) has been designed to support the development of a fiber-optic Thomson-scattering system at LLE. Thomson scattering will be used to characterize the growth of electron plasma waves in pump–probe experiments that last less than 25 ps. The spectrometer was designed to match the 1-ps temporal resolution of the Rochester Optical Streak System 8200 (Ref. 4). The spectrometer provides a 100-nm spectral field of view centered at the 527-nm Thomson-scattering probe wavelength with a 0.8-nm spectral resolution. Light from the plasma-wave experiment will be coupled to the spectrometer using a gradient-index fiber optic. The fiber has a 50-μm core diameter and a 0.2 (*f*/2.5) numerical aperture. The input signal is collimated by a 225-mm-focal-length, color-corrected doublet lens operating at *f*/2.9. Angular dispersion is provided by a 300-g/mm transmission grating that generates 40 ps of pulse-front tilt. A 34-element reflective echelon optic with 2.2-mm step widths and 174-μm step heights is used to improve the achievable temporal resolution to 1.2 ps. Individual spectrometer segments focus to the streak camera at *f*/100, producing diffraction-limited spot sizes of 55-μm full width at half maximum (FWHM). Figure 147.38 shows how the echelon step width was optimized to improve temporal resolution while maintaining spectral resolution close to the performance of the nominal full-aperture system.

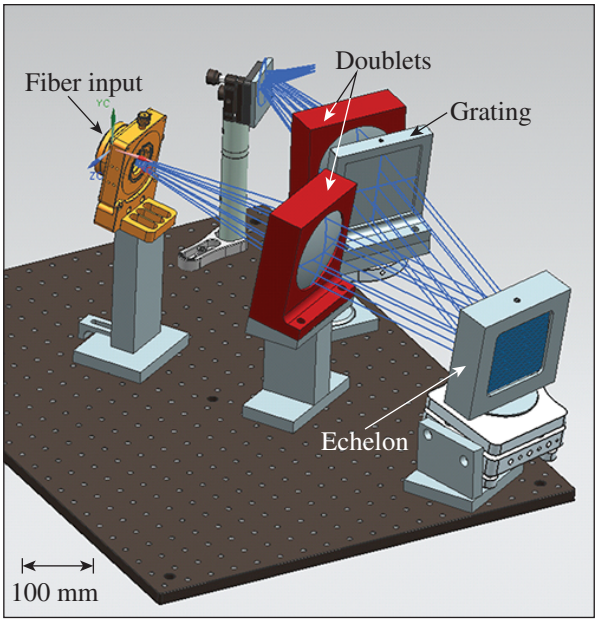

Figure 147.37
CAD model of the spectrometer layout. A pair of *f*/2.9 doublets collimate and focus the dispersed input from a 50-μm-core fiber optic. The PFT from the 300-g/mm transmission grating is reduced by using a 34-element reflective echelon optic.

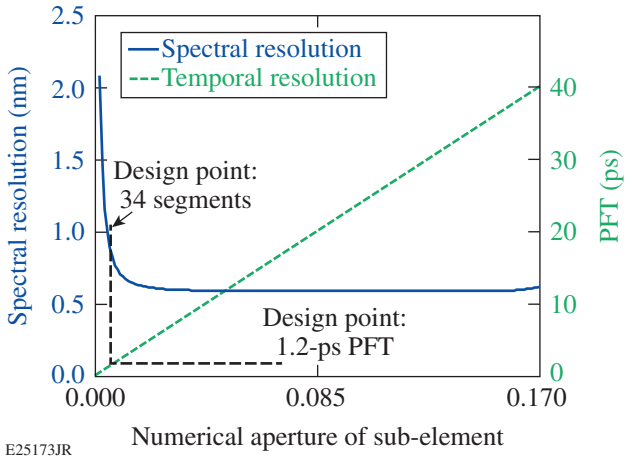

Figure 147.38
Spectral resolution is determined by convolving the modeled imaging-performance parameters and multiplying by linear dispersion. The overall beam size was selected based on the geometric limitations of the imaging optics. Temporal resolution was improved by segmenting the full beam into properly delayed sub-elements. The design point represents a compromise between these factors, resulting in 0.8-nm spectral resolution, 1.2-ps temporal resolution, and *f*/2.9 throughput.

Conclusions

This article presents a novel spectrometer design that decouples the relationship between throughput and pulse-front tilt. An echelon optic is used to segment the aperture of the spectrometer into a series of sub-elements that are optically and temporally co-aligned. This technique makes it possible to optimize the spectral resolution, throughput, and temporal resolution simultaneously.

ACKNOWLEDGMENT

This material is based upon work supported by the Department of Energy National Nuclear Security Administration under Award Number DE-NA0001944, the University of Rochester, and the New York State Energy Research and Development Authority. The support of DOE does not constitute an endorsement by DOE of the views expressed in this article.

REFERENCES

1. J. Hebling, Opt. Quantum Electron. **28**, 1759 (1996).
2. S. Akturk, X. Gu, P. Bowlan, and R. Trebino, J. Opt. **12**, 093001 (2010).
3. A. Visco, R. P. Drake, D. H. Froula, S. H. Glenzer, and B. B. Pollock, Rev. Sci. Instrum. **79**, 10F545 (2008).
4. Sydor Instruments, LLC, Rochester, NY 14624.